DOI: 10.17344/acsi.2021.7289 *Acta Chim. Slov.* **2022,** *69,* 336–348

Scientific paper

Removal of Diazo Dye Direct Red 28 and Tetra Azo Dye Direct Black 22 Using Synthesized Magnetic Kaolin Supported Zinc Ferrite

Serap Fındık*

Chemical Engineering Department, Engineering Faculty, Hitit University, Kuzey Yerleşkesi, Cevre Yolu Bulvarı, 19030, Çorum, Turkey

** Corresponding author: E-mail: serapfindik@hitit.edu.tr*

Received: 11-21-2021

Abstract

The presence of dye molecules in water resources has harmful effects on environment. Therefore, it is important to remove dyes from wastewater using eco-friendly materials. In this study, adsorptive removal of diazo dye Direct Red 28 (DR-28) and tetra azo dye Direct Black 22 (DB-22) was investigated by using a new composite, kaolin supported zinc ferrite (KZF) as adsorbent. Characteristics of the composite, KZF were determined using various techniques such as FTIR, SEM, XRD, VSM, and EDS/Mapping. The adsorption of DR-28 and DB-22 on KZF was studied as a function of contact time, initial dye concentration, adsorbent amount, temperature, initial pH of the solution as well as the heat treatment of the composite. The removal of DR-28 was found to be 92.4% for the KZF concentration of 1g/200mL, initial dye concentration of 20 mg/L, contact time of 120 min at original pH and 21 °C. On the other hand the removal of DB-22 was found to be 91.7% under the same conditions at 40 °C. The results showed that Langmuir isotherm is suitable for the adsorption of DR-28 and DB-22 on KZF under given conditions. It was found that adsorption of DR-28 on KZF was exothermic while that of DB-22 was endothermic. The enthalpy changes (ΔH^0) for the adsorption of DR-28 and DB-22 dyes on KZF were found to be –24.59 kJ/mol and 61.95 kJ/mol respectively. ΔS^0 for the adsorption of DR-28 dye was found to be negative while ΔS^0 for the adsorption of DB-22 was positive. The kinetic data fitted well to the pseudo second order model for the adsorption of DR-28 and DB-22 on KZF composite. These results showed that the prepared adsorbent KZF could be used as an adsorbent for the efficient removal of anionic dyes.

Keywords: Adsorption, direct black 22, direct red 28, magnetic kaolin, zinc ferrite

1. Introduction

Dyes are chemical compounds used to color products in many fields such as textile, leather, paper, rubber, printing and plastic.[1] Dyes in wastewater are dangerous and negatively affect the water quality. The discharge of wastewater containing dyes into water resources causes a decrease in gas solubility, light and oxygen permeability, and therefore a decrease in photosynthesis. It also affects aquatic life and human life due to its carcinogenic and mutagenic effects.[1–4] Dyes entering the human body through the food chain cause diseases such as dizziness, jaundice, diarrhea, and nausea. They also damage to organs such as kidney, brain and liver.[1,3]

Dyes can be divided into two categories: natural and synthetic dyes. With the increase in dye consumption, natural dyes have been replaced by synthetic ones. Synthetic dyes consist of three parts: chromophoric groups, auxochromes and conjugated aromatic structures. Chromophoric groups are unsaturated and they consist of atoms or groups of atoms that allow the light to be absorbed.[5] Dyes can also be classified according to the chromophoric groups: Azo, Anthraquinone, Indigoid, Nitroso, Nitro, and Triarylmethane.[1,6] Azo dyes are characterized by the number of azo bond groups such as monoazo, diazo, triazo, polyazo and azoic. Polyazo dyes are complex structures and contain three or more azo groups in the same molecule.[7]

Direct red 28 (DR-28, known as Congo red) and Direct black 22 (DB-22) are widely used in textile, paper and plastic industries.[8,9] DR-28 contains two azo groups and DB-22 contains tetra azo groups. Both DR-28 and DB-22 are anionic dyes.[7] DR-28 and DB-22 in wastewater damage the environment due to their carcinogenic and toxic properties. Therefore, DR-28 and DB-22 containing

wastewater should be treated before being released into environment.

Different treatment methods such as coagulation-flocculation[10], Fenton[11], ozonation[12], UV[13], photocatalytic process[14], and adsorption[15] are applied to remove dyes from aqueous solutions. Among these methods, adsorption has gained importance in recent years since it becomes more economical with cheap, simple, and efficient adsorbents. Natural adsorbents such as clinoptilolites, montmorillonites, esmectites, kaolinites, and bentonites have been successfully used for adsorption.[16]

Kaolin has a great potential in the removal of dyestuffs from wastewater thanks to its chemical and mechanical stability, high cation exchange capacity, adsorption ability, unique structural properties as well as its low cost, high efficiency, and abundance.[17,18] On the other hand, the surface properties such as surface area and surface exchange sites of kaolin should be improved to increase the adsorption capacity. For this purpose, physical and chemical processes such as milling, heat treatment, acid treatment, and alkaline treatment can be applied. While alkaline treated kaolin has a small surface area, kaolin with a large surface area can be obtained by acid treatment. However, acid treatment is difficult due to the inert nature of kaolin. Metakaolinite is obtained by the calcination of kaolinite.[17,19]

Magnetic adsorbents are new generation adsorbents with high adsorption capacity and speed. Compared to other adsorbents, magnetic adsorbents have some advantages such as less production cost, easy separation from solution, low diffusion resistance, and large surface area.[4] Among the magnetic nanoparticles, spinel ferrites with the chemical composition of MFe_2O_4 (M=Cu, Mn, Zn, Mg, Co, Ni and other metals) have been extensively studied so far due to their special properties, where oxygen ions (O^{2-}) make a cubic structure, Fe^{3+} cations occupy half of the octahedral holes and M^{2+} ion is a divalent cation and place in the eight holes of the tetrahedral.[2] Zinc, cobalt, and nickel ferrites are widely used as a magnetic support thanks to their high saturation magnetization intensity and excellent mechanical strength.[20]

The addition of inorganic particles such as spinel ferrite to the matrix of kaolinites can improve the adsorption capacity and facilitate its separation from the aqueous solution by an external magnet. This process improves both the physical and chemical properties of kaolinite and provides high adsorption capacity by preventing agglomeration of inorganic nanoparticles.[21]

The aim of this study was to investigate the performance of magnetic kaolin supported zinc ferrite as an adsorbent for the removal of diazo dye DR-28 and tetra azo dye DB-22 from aqueous solutions. The prepared adsorbent was characterized using FTIR, SEM-EDS, XRD and VSM techniques. In order to determine the optimum adsorption parameters, the effect of process variables such as heat treatment of the composite KZF, adsorbent amount, initial dye concentration, contact time, initial pH of the solution, and temperature have been investigated. After optimization of the effective factors, the kinetics and isotherm of the adsorption were investigated. A thermodynamic study was realized to understand the behavior of the adsorption process.

2. Materials and Methods

2. 1. Materials and Equipments

The kaolin clay with a particle size of 28 **μ** was procured from a company in Balıkesir, Turkey. It was a commercial product and used without purification. DR-28 was supplied from Isolab, DB-22 (commercial name Direct Black 22 VSF 1600) from a company named "HNY" in Turkey, and $FeSO_47H_2O$ and $ZnSO_47H_2O$ from Merck.

A magnetic stirrer (HSD-180), pH meter (C561, Consort), centrifuge (Nuve, NF 200) and oven (Proterm, PLF 120/5) were used in the study. UV- spectrofotomoter (Hach, DR-2400) was used to measure the absorbance of the dye samples.

2. 2. Preparation of the Adsorbent

The composite kaolin/Zn/Fe was prepared by chemical coprecipitation method. First, iron II sulphate heptahydrate ($FeSO_4.7H_2O$) and zinc sulphate heptahydrate ($ZnSO_4.7H_2O$) with a molar ratio of 2:1 were dissolved in 200 ml distilled water. Then, kaolin clay was added to the solution and heated to 65–70 °C while stirring with a magnetic stirrer. The mixture was stirred for 30 min. 3M NaOH solution was added dropwise to the solution, and pH of the solution was adjusted to 12. After addition of NaOH solution, stirring was continued for one hour at 100 **°C.** The prepared composite was left for one day at room conditions and then placed in water bath for 4 h at 95 **°C.** After that, it was dried at 95 **°C** for 90 h. Finally, the dried composite was heat treated at 200 °C for **3** h. The composite with and without heat treatment were coded as KZF-200 and KZF, respectively, and the raw kaolin as K.

2. 3. Characterization of Adsorbent

The adsorbents used in the study were characterized by XRD, FTIR, SEM, EDS, and VSM. Powder X-ray diffraction (XRD) patterns of the adsorbent were recorded using Rigaku Smart Lab with Cu-Kα radiation at 40 kV and 30 mA to determine the crystalline structure of the samples. The samples were scanned from 5°–90° at a rate of 2°/min, and with a step size of 0.01. Fourier transform infrared (FTIR) (PerkinElmer, Spectrum Two) spectroscopy analysis was performed in the range of 400–4000 cm^{-1} to identify the functional groups of the adsorbents before and after adsorption. SEM and EDS analysis were performed using Jeol, JSM 7001F. Magnetic saturation was

measured using a vibrating sample magnetometer (VSM Lake Shore 7407).

2. 4. Adsorption Experiments

A stock solution of dye was prepared using distilled water. Standart dye solutions with known concentration were prepared using stock solution, then absorbance values of the standard dye solutions were recorded using UV-spectrophotometer (Hach, DR-2400). The absorbance of DR-28 and DB-22 solutions was recorded at 497 nm and 481 nm, respectively. The calibration graph was drawn using the absorbance values of the standard solutions.

For the adsorption experiments, the desired amount of adsorbent was put in 200 ml of dye solutions and the sample was magnetically stirred continuously at 600 rpm. The stirring rate was constant in all experiments. The dye solutions were kept at room temperature (21 °C) in all experiments except those in which the effect of temperature was investigated. pH was adjusted with HCl and NaOH solutions to 6.5–9. The original pH of the dye solution was ≈7.4. In the experiments, the amount of adsorbent and the initial dye concentration were changed in the range of 0.6–1.2 g/200mL and 20–50 mg/L, respectively. All the experiments were repeated twice. Process variables such as the heat treatment of the composite KZF, contact time, pH, the initial concentration of dye solution, amount of adsorbent, and temperature were investigated in the study. The samples were withdrawn from the reaction mixture and centrifuged at 5000 rpm for 10 minutes to remove the adsorbent. The absorbance of the samples was measured to find the concentration of dye.

Efficiency of the dye removal, (R) was calculated using Eq. (1).

$$R, \% = [C_o\text{-}C_t)/C_o]*100 \quad (1)$$

Equation 2 gives the adsorption capacity of the adsorbent:

$$q_e= ((C_o\text{-}C_e)*V)/W \quad (2)$$

where q_e is the adsorption capacity of the adsorbent at equilibrium (mg/g), C_o is the initial concentration of dye, C_t is the concentration of dye at any time (mg/L), C_e is the concentration of dye at equilibrium (mg/L), V is the volume of the dye solution (L), and W is the weight of the adsorbent (g).

3. Results and Discussion

3. 1. Adsorbent Characterization

The SEM and EDS/Map analyses were used to examine the structure and distribution of elements at the surface of the adsorbent. SEM, EDS spectra and EDS mapping images of the composite KZF are given in Fig. 1. As shown in Fig. 1-a, KZF has an irregular and porous surface structure. The EDS/Map analyses were used to determine the Zn and Fe particles in the kaolin layers, and the results confirm that there are Fe and Zn ions in the structure of KZF. KZF includes iron (7.1%), zinc (4.8%), silisium (6.2%), oxygen (45%), sodium (16.7%), aluminum (4.1%), carbon (9.6%) and sulphur (5.3%). According to the results of EDS analysis, kaolin was successfully loaded with Fe and Zn, and the elements were observed to distribute uniformly.

As shown in Fig. 2, the bands found at ~3690 and 3620 cm^{-1} are the typical bands for the ordered structure of kaolin. The bands at ~3690 cm^{-1} and 3620 cm^{-1} are related to the OH and H-O-H stretchings, respectively.[19] The peaks at 1117, 1030, and 1001 cm^{-1} may be due to Si-O stretching.[2,19] The peak at 910 cm^{-1} can be attributed to Al-OH-Al stretching vibration.[22] The peaks at 796, 752 and 691 cm^{-1} may be due to the tensile vibrations of Si-O-Si, Si-O-Al and Si-O-Mg and the bending vibrations of SiO in the structure of kaolin.[2]

The peaks detected at 910, 940, 1001, 1030, and 1117 cm^{-1} in the spectrum of kaolin disappeared in the FTIR spectra of KZF and KZF-200. The bands of KZF and KZF-200 (752, 796, 3620 and 3690 cm^{-1}) were similar to those of the raw kaolin but transmittance of these bands was higher than that of the kaolin. The weak and disappeared peaks showed the change in the structure of kaolin. This can be interpreted as the Al^{3+} crystals in the kaolin structure were replaced by Fe^{3+}.[19] There were new bands at 1440, 1100 and 980 cm^{-1} in KZF and KZF-200. The peaks at 1440, 1100 and 980 cm^{-1} may be due to O-H bending, C-O stretching and C=C bending, respectively.

When the FTIR spectra of KZF were compared with the FTIR spectra taken after the adsorption of DR-28 or DB-22 on KZF, it was seen that both had the same bands except the peaks at 1440 and 1100 cm^{-1}. After the adsorption of DR-28 and DB-22 by KZF, the peaks at 1440 and 1100 cm^{-1} disappeared. The transmittance of KZF after the adsorption of dye was lower than that of KZF. This indicates that the functional groups of KZF were involved in the dye adsorption.[23] After the dyes were adsorbed by KZF, some of the peaks disappeared and the range of some of the absorption peaks changed. This may be due to the interaction between the functional groups in the KZF and the dye molecules.[2]

Fig. 3 shows XRD patterns of K, KZF, and KZF-200. As seen in Fig. 3, kaolin has three intense diffraction peaks at 2θ at 12.34°, 24.87° and 26.61°. These peaks are associated with the presence of kaolinite. Similar diffraction peaks were reported by Meroufel et al.[8] and Niu et al.[24] The diffraction peak at 20.86° is associated with quartz.[8] In addition to the typical peaks of kaolin, new peaks at 19°, 28.9°, **32**.1°, 33.8°, 35°, 48.7°, 54.6°, 59.5° and 62° were observed in XRD spectra of KZF and KZF-200. According to the PDF card, peaks appear at 19°, 28.9°, 35°, 59.5° and 62°

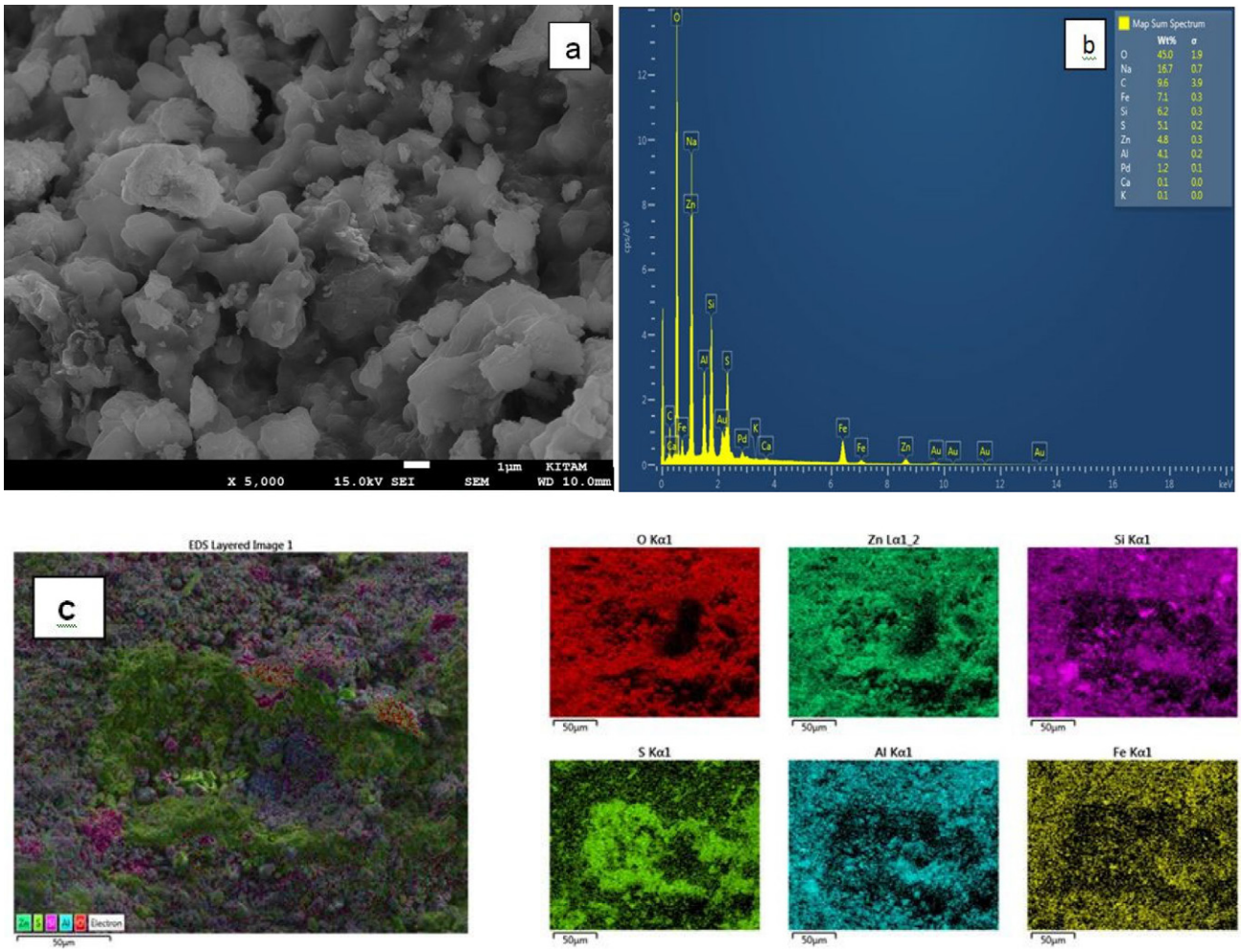

Fig. 1. The SEM (a), EDS spectra (b), EDS Mapping analyses (c) for KZF composite The functional groups of the kaolin, KZF, KZF-200 and DR-28 or DB-22 adsorbed KZF were determined using FTIR analysis. The related FTIR spectra are shown in Fig. 2.

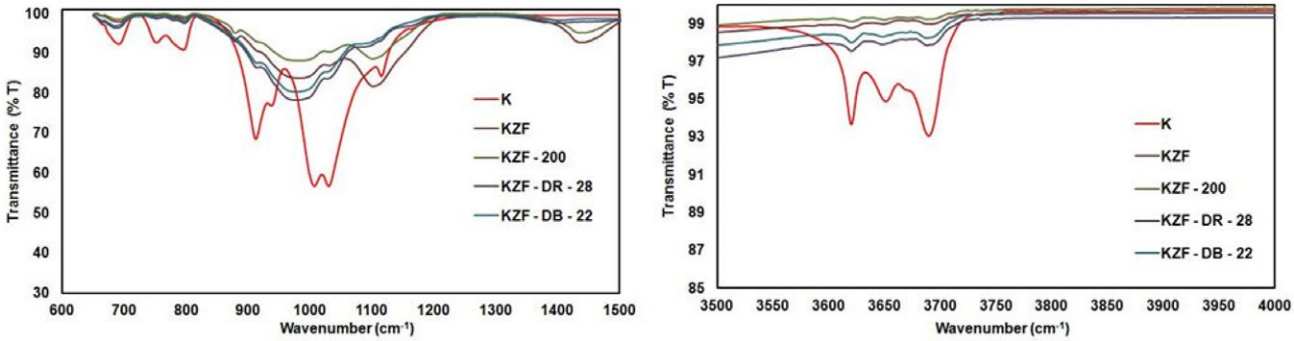

Fig. 2. FTIR spectra of K, KZF, KZF-200, and dye adsorbed KZF

match well with PDF card 00-010-0467 (Franklinite, $ZnFe_2O_4$).

The peaks at 28.9° and 33.8° indicate that these composites contain typical zinc oxide, magnetite, and zinc ferrite structures. The diffraction peak at 28.9° indicates the successful introduction of Zn to Fe spinel after synthesis. The peak at 35° shows the development of the spinel phase indicating a zinc ferrite formation in the composite.[25]

The magnetic behavior of KZF at 298K was investigated by VSM analysis**.** The result is shown in Fig. 4. As can be seen in the Fig. 4, the amount of magnetic saturation for the KZF was determined as 3.3 emu/g. The low value of magnetic saturation for KZF is due to the fact that the magnetite was covered by the kaolin.[26] However, KZF can be separated from the solution using a permanent magnet. The magnetization curve of KZF exhibited zero

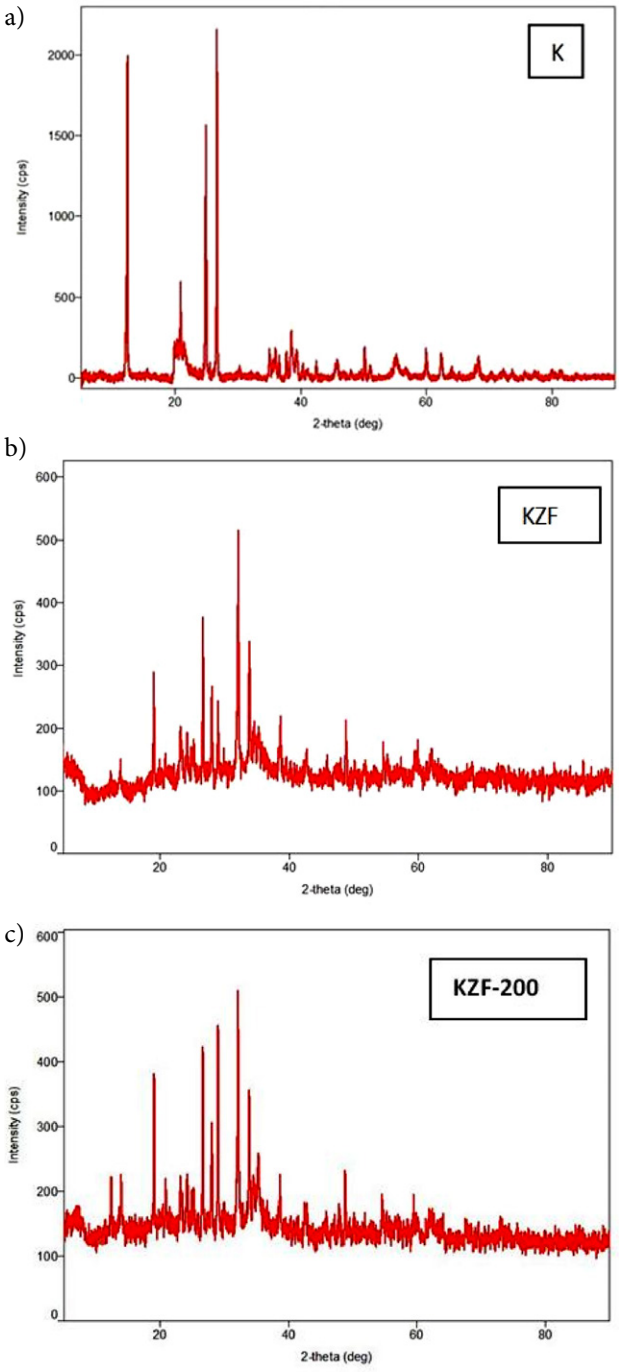

Fig. 3. XRD spectra of K, KZF and KZF-200

coercivities and remanences indicating a superparamagnetic behavior of the sample at room temperature.[27]

3. 2. Effect of Heat Treatment

KZF and KZF-200 composites were considered to investigate the effect of the heat treatment on dye removal performance of the composites. The experiments were

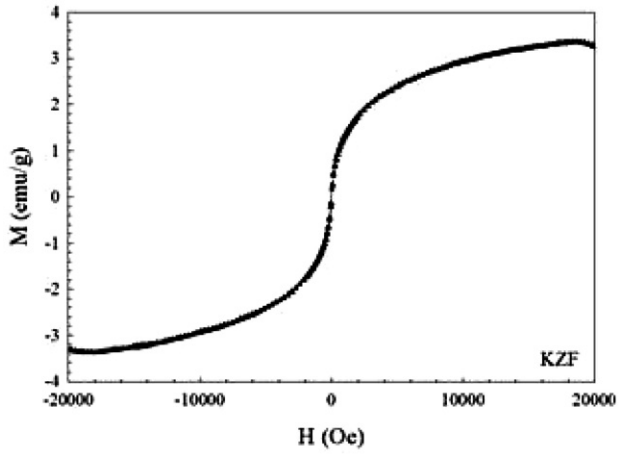

Fig. 4. VSM analysis of KZF at room temperature

performed at an initial dye concentration of 30 mg/L, with an adsorbent amount of 0.6g/200mL, at 21 °C and original solution pH of ≈7.4. As seen in Fig. 5, lower removal rates were obtained for both DR-28 and DB-22 in the experiments with kaolin compared to those with KZF and KZF-200.

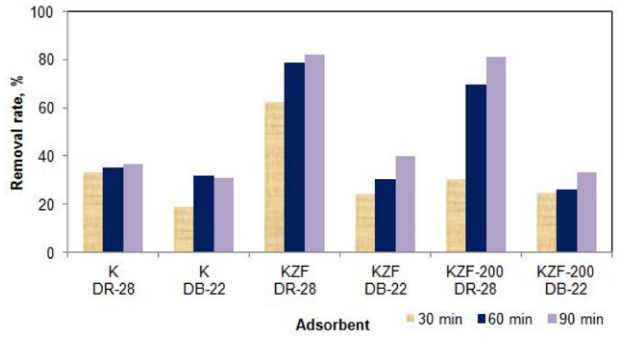

Fig. 5. Effect of the heat treatment on the removal of (a) DR-28 and (b) DB-22 (initial concentration: 30 mg/L, temperature: 21 °C, adsorbent amount: 0.6g/200mL, initial pH: original)

DR-28 removals at the end of 90 minutes were found to be 82.3% and 81.1% in the experiments with KZF and KZF-200, respectively. The removal rates in the contact time of 90 min were almost the same. However, in the contact times of 30 and 60 minutes, KZF provided a higher DR-28 removal than KZF-200. In the experiments, DB-22 removal was found to be higher for the composite KZF. In the contact time of 90 min, the removals of DB-22 were found to be 40% and 33.3% in the experiment with KZF and KZF-200, respectively. Therefore, KZF was chosen as the adsorbent, and the effect of the other parameters was examined using KZF.

The heat treatment temperature affects the structure of the composite. In one study, Olusegun and Mohallem[21] studied adsorption of Congo red using synthesized kaolinite supported $CoFe_2O_4$ nanoparticles calcined at different

temperatures. Adsorption capacity of the composite without calcinations was higher than the calcined composite at 700 °C. Calcination temperature up to 700 °C resulted in structural damage to kaolinite.

As shown in Fig. 2, KZF and KZF-200 had the same peaks, but the transmittance of KZF was lower than that of KZF-200. The kaolinite had a disordered structure at lower temperatures due to dehydroxylation.[28]

The removal rate of DR-28 was found to be higher than that of DB-22. DR-28 has two azo bonds, on the other hand, DB-22 has tetra azo bonds. The higher the number of azo bonds, the higher the stability of dye, which makes the dye removal difficult.

In addition, the molecular weight of the tetra azo dye DB-22 was higher than that of the diazo dye DR-28. The molecular weights of DB-22 and DR-28 were 1084 g/mol and 696.67 g/mol, respectively. The distribution of dyes in water increases with the increase of the molecular weight of the azo dyes, which causes a decrease in the rate of azo dye degradation.[7]

3. 3. Effect of Adsorbent Amount

In the present study, the effect of adsorbent amount on dye removal was also investigated. Experiments were done with a various amounts of adsorbent at the initial concentration of 30 mg/L, at 21 °C and original pH. Fig. 6 shows the effect of adsorbent amounts on the removal of DR-28 and DB-22. The removal of DR-28 increased with increasing KZF amount from 0.6g/200mL to 0.8g/200mL then remained constant. DR-28 removals at the end of 90 min were found to be 89.7%, 90.2% and 90.1% for the KZF amounts of 0.8, 1, and 1.2g/200mL respectively. At the end of 30 min, the removals of DR-28 were found to be 76.4% and 88.9% in the KZF amounts of 0.8g/200mL and 1g/200mL respectively. Therefore, 1g/200mL of KZF was chosen as the optimum adsorbent amount.

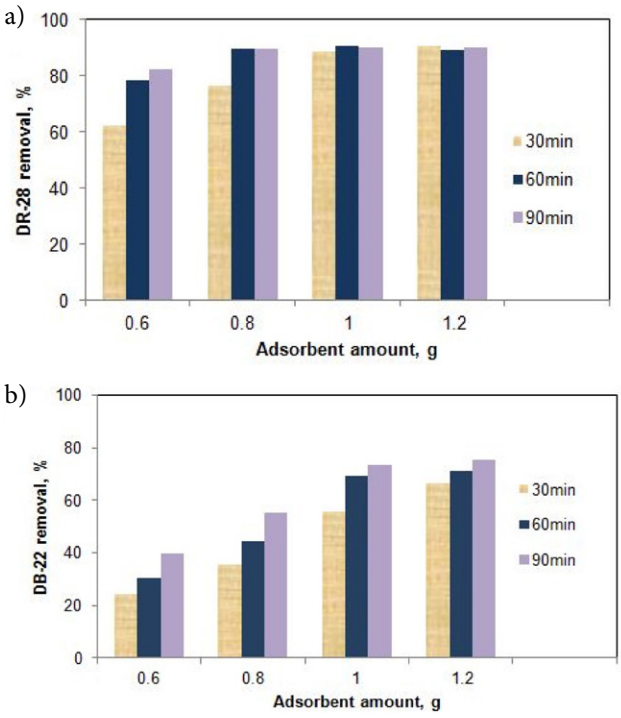

Fig. 6. Effect of KZF amount on the removal of (a) DR-28 and (b) DB-22 (initial concentration: 30 mg/L, temperature: 21 °C, initial pH: original)

The removal of DB-22 increased with the increasing the amount of adsorbent within the range of 0.6g/200mL–1.2g/200mL. The removals of DB-22 at the end of 90 min, were 40%, 55.3%, 73.2%, and 75.4% in the KZF amounts of 0.6, 0.8, 1, and 1.2g/200mL respectively. There was no significance difference between the DB-22 removals of 1g/200mL and 1.2g/200mL KZF.

DB-22 removal was lower than the removal of DR-28 under the studied conditions. As mentioned in the previous section, removal of tetra azo dyes is more difficult than that of diazo dyes.

The removal of DR-28 and DB-22 increased with the increasing adsorbent amount due to the increase in surface area and number of active sites. After the optimum adsorbent amount, the effective active surface area decreased due to the accumulation of adsorbent particles, and as a result, the removal rate remained almost constant. Nicola et al.[27] investigated the adsorption of Congo red using magnetic mesoporous silica. The removal of Congo red increased with increasing the adsorbent amount from 0.5 to 1g/L and after 1g/L adsorbent amount removal rate remained nearly constant. Similarly, Boushehrian et al.[2], reported that the removal of methylene blue and methyl violet remained almost constant after the adsorbent dosage of 1.5g/L. Cao et al.[29] investigated the adsorption of reactive brilliant red using magnetic Fe_3O_4/chitosan nanoparticles and reported that the optimum adsorbent amount was 0.6 g/L, and after the optimum adsorbent amount, the removal rate was almost the same. In another study, Karthikeyan et al.[30] studied the adsorption of phosphate and nitrate ions from water using magnetic kaolin (MK) chitosan beads and reported that, the removal of phosphate and nitrate increased with the increasing amounts of MK-chitosan beads due to the increase in reactive vacant sites of the adsorbent surface. Moreover, they also reported that, there was no significant change in the removal rate at the adsorbent amounts greater than 100 mg. Koohi et al.[31] also reported similar results. They found that the removal efficiency of Congo red increased with the increasing amounts of Fe_3O_4/NiO due to the increase in the active surface area, and after the adsorbent amount of 15 g/L, no significant change was observed in the removal rate. The decrease in the surface area due to the aggregation of particles causes a decrease in the adsorption capacity. Esvandi et al.[3] examined the adsorption of sunset yellow and Nile blue using magnetic nanoparticle, and reported that the removal efficiency increased when the adsorbent amount was increased from 0.4 g/L to 1 g/L (optimum adsorbent

amount), and after the adsorbent amount of 1 g/L, the removal rate remained constant. In another study, Mahmoodi et al.[32] investigated the adsorption of direct black 22 using polyaminoimide homopolymer. They reported that removal of direct black 22 increases with increasing adsorbent amount due to increased adsorbent surface and availability of more sites.

3. 4. Effect of Initial pH

The pH of solution is an important parameter affecting the adsorption of dye onto the adsorbent. DR-28 is a diazo dye which changes colour at low pHs due to protonation of its amino groups. The red color of DR-28 changes to bluish color below the pH 5.[8,21,33] For this reason the effect of pH was not investigated under strong acidic conditions.

The effect of pH on the removal of DR-28 and DB-22 was studied at the initial pHs of 6.5, ≈7.4, 8.5, and 9. ≈7.4 is the original pH of the dye solution. The results are presented in Fig. 7. The pH of the dye solution was adjusted at the beginning of the experiment and not controlled during the adsorption process.

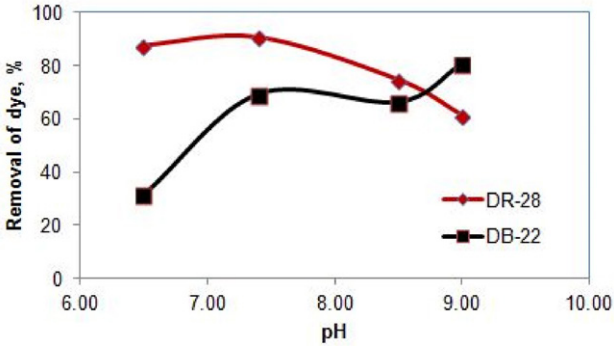

Fig. 7. Effect of initial pH of the dye solution on the removal of DR-28 and DB-22 (initial concentration: 30 mg/L, temperature: 21 °C, adsorbent: KZF, adsorbent amount: 1g/200mL, contact time: 60 min)

The removal rate of DR-28 increased from 87.5% to 90.5% when the pH of the solution was increased from 6.5 to 7.4. After the original pH, the removal rate decreased with the increase in solution pH, which could be attributed to the de-protonation of the adsorbent surface. Similarly, Koohi et al.[31] reported that the removal of Congo red decreased as the pH was increased after the optimum pH. They also reported that, the adsorption capacity gradually decreased, due to the repulsion between the Congo red ions and the adsorbent molecules. Das et al.[33] investigated the effect of pH on the decolorization of Congo red and reported that, highly acidic and highly basic conditions were not suitable for the decolorization of Congo red solution. They obtained the maximum decolorization of Congo red at pH 7.

The removal of DB-22 increased when the pH was increased from 6.5 to 7.4 (original pH). At the pHs of 7.4 and 8.5, there was no significant change in the removal rate. The removal of DB-22 was found to be 80.4% in pH 9. Sun et al.[34] reported similar result for the adsorption of anionic dye reactive red 123 and explained the effect of pH on the adsorption by electrostatic interaction between the adsorbent and the dye molecules. Based on these results, it can be asserted that the adsorption mechanism is not dependent solely on electrostatic interaction. The molecular structure of dyes may also affect the adsorption process.

3. 5. Effect of Temperature

In the study, the effect of temperature on dye removal was also investigated to reveal whether the adsorption process is exothermic or endothermic. The experiments were done at different temperatures at the initial concentration of 30 mg/L, with the adsorbent amount of 1g/200mL and the contact time of 60 min at original pH. Fig. 8 presents the effect of temperature on the removal of DR-28 and DB-22.

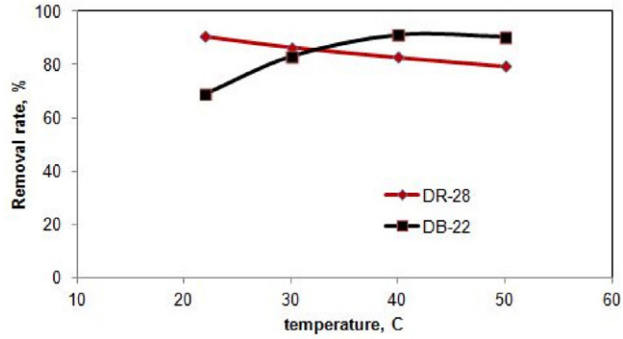

Fig. 8. Effect of temperature on the removal of DR-28 and DB-22 (pH: original, initial concentration: 30 mg/L, adsorbent: KZF, adsorbent amount: 1g/200mL, contact time: 60 min)

The removal of DR-28 decreased with the increasing temperature. This result shows that, the adsorption of DR-28 on KZF was exothermic. As the temperature increases, the tendency of the dye adsorbed on the adsorbent surface to separate from the surface increases.[2] According to Esvandi et al.[3], the adsorption efficiency decreases with increasing the temperature due to the desorption of dye molecules from the adsorbent surface. Maqbool et al.[35] investigated the removal of Congo red using free biomass, Na-Alg/CH and PPY/CH conjugates. It was found that the removal of Congo red decreased with increasing temperature due to the weakened Van der Waals force and the H-bonding between the adsorbent and the sorbate.

On the other hand, the removal of DB-22 increased with increasing the temperatures up to 40 °C. The removals of DB-22 at the initial concentration of 30 mg/L and the contact time of 60 min were found to be 69.2%, 83.2% and 91.3% at the solution temperatures of 21, 30, and 40 °C, respectively. After 40 °C, the removal rate remained almost

constant. So, the adsorption of DB-22 on KZF is an endothermic process. Magdy et al.[19] reported similar results for the adsorption of Direct Red 23. The mobility of dye molecules changes with temperature. As the temperature of the solution increases, the mobility of the dye molecules increases and as a result, the number of dye molecules interacting with the free active sites on the composite surface increases.

Based on the experimental results, it can be asserted that the optimum temperatures for the removal of DR-28 and DB-22 were 21 °C and 40 °C, respectively. For this reason, the experiments examining the effect of initial dye concentration were carried out at these optimum temperatures.

3. 6. Effect of Initial Dye Concentration and Contact Time

In the study, the effects of initial dye concentration and contact time on dye removal were also investigated. The experiments were done within an initial concentration range of 20–50 mg/L with an adsorbent amount 1g/200mL, at original pH. The experiments examining the effect of contact time and initial dye concentration were carried out at the optimum temperature values specified in the previous section (i.e., 21 °C for DR-28 and 40 °C for DB-22). Fig. 9 presents the effect of initial dye concentration and contact time on the removal of DR-28 and DB-22.

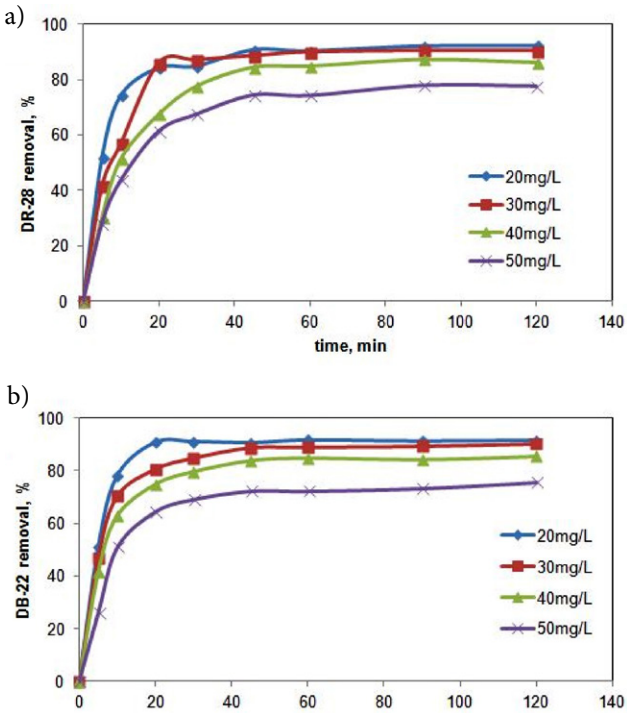

Fig. 9. Effect of initial dye concentration and contact time on the removal of (a) DR-28 and (b) DB-22 (pH: original, temperature: 21 °C (for DR-28), 40 °C (for DB-22), adsorbent: KZF, adsorbent amount: 1g/200mL)

The experimental results showed that the removal rates of DR-28 and DB-22 were faster for the first 20 min, and then slowed down. The removal rate was almost constant after the contact time of 30 min. At the beginning of the adsorption process, active surface area is high. As the time progresses, empty areas begin to fill and the appropriate surface area decreases due to saturation with dye molecules. Accordingly, the rate of the adsorption process decreases and reaches an equilibrium.[2,30]

As seen in Fig. 9, the removal of DR-28 and DB-22 decreased with the increasing initial dye concentrations. The removals of DR-28 for the contact time of 120 min were found to be 92.4%, 89%, 86% and 77% at the initial dye concentrations of 20, 30, 40, and 50 mg/L, respectively. Similar result was obtained for DB-22. The removals of DB-22 were found to be 91.7%, 90.2%, 85.5%, and 75.6% at the initial DB-22 concentration of 20, 30, 40, and 50 mg/L respectively. Mass transfer occurs due to the concentration difference between the aqueous phase and the adsorbent surface. Initial concentration of the dye solution is the driving force for mass transfer. The removal rate decreases with the increasing initial dye concentration due to the decrease in the number of active sites of the adsorbent.[16] Magdy et al.[19] reported similar results. As the dye concentration increases, the adsorbent reaches saturation quickly for a fixed amount of adsorbent, and the active surfaces are covered with dye molecules. According to Sanad et al.[36], at high dye concentrations, the unit mass of the adsorbent is exposed to more dye molecules. As a result, the active sites are gradually filled until they reach saturation causing a decrease in removal efficiency. Boushrean et al.[2] examined the effect of initial concentration on the removal of methylene blue and methyl violet and reported that the ratio of the active surface area of the adsorbent to the dyes in the solution was high at low dye concentrations, and for this reason, all the dye molecules interacted with the adsorbent, and thus a higher removal efficiency was achieved.

3. 7. Adsorption Isotherms

The adsorption equilibrium data collected at the dye concentrations of 20–50 mg/L were fitted by common isotherms Langmuir and Freundlich models. The Langmuir isotherm model assumes that the adsorbate is coated in a monolayer on the homogeneous adsorbent surface, and the adsorption takes place only at the active sites on the adsorbent. The Freundlich equation is an empirical equation used to describe heterogeneous systems.[29]

Langmuir and Freundlich models are given in Eqs. (3) and (4), respectively. [2,22,37]

$$\frac{C_e}{q_e} = \frac{C_e}{q_{max}} + \frac{1}{q_{max} K_L} \quad (3)$$

$$lnq_e = lnk_f + \frac{1}{n} lnC_e \quad (4)$$

$$R_L = \frac{1}{1+K_L C_o} \quad (5)$$

where q_{max} is the adsorption capacity (mg/g), K_L is the adsorption energy (L/g), and K_f and n are the Freundlich constants.

The value of R_L specifies whether the adsorption process is irreversible (R_L=0), desirable (0<R_L<1), linear (R_L=1) or undesirable (R_L>1). The value of n determines whether the adsorption process is linear (n=1), physical (n>1) or chemical (n<1).

The adsorption isotherm models were calculated at the initial dye concentrations of 20–50 mg/L. The other factors, such as initial pH, adsorbent amount, and temperature were kept constant. For DR-28 and DB-22, the initial pH was original pH, and the amount of the adsorbent KZF was 1g/200mL. While the parameters such as adsorbent amount and pH were the same for both dyes, the temperature was 21 °C for DR-28 and 40 °C for DB-22.

The values and constants of the Langmuir and Freundlich isotherm models for DR-28 and DB-22 are given in Table 1. The results of the Langmuir adsorption isotherm models for DR-28 and DB-22 are shown in Fig. 10 and Fig. 11, respectively.

The values of R^2 for the Langmuir model were found to be 0.9969 and 0.9926 for DR-28 and DB-22, respectively. The values of R^2 for the Freundlich model were found to be 0.9308 and 0.8381 for DR-28 and DB-22, respectively. DR-28 and DB-22 adsorptions were found to be in a good agreement with the Langmuir isotherm. The calculated R_L values of DR-28 and DB-22 were between 0 and 1. Based on these results, it can be asserted that the adsorption process was desirable.

Table 1. Langmuir and Freundlich isotherm parameters for the adsorption of DR-28 and DB-22 (pH: original, adsorbent: KZF, adsorbent amount: 1 g/200mL, temperature: 21 °C for DR-28, 40 °C for DB-22)

Isotherm	Constants	DR-28	DB-22
Langmuir	q_{max} mg/g)	7.640	8.404
	K_L (L/mg)	0.722	0.605
	R^2	0.9969	0.9926
	R_L	0.027–0.064	0.032–0.076
Freundlich	n	3.59	3.03
	K_f (mg/g)	3.71	3.53
	R^2	0.9308	0.8381

3. 8. Adsorption Thermodynamics

Thermodynamic parameters (ΔG^0, ΔH^0, ΔS^0) were calculated using the Eqs. (6), (7), and (8). The values of ΔH^0 and ΔS^0 were calculated from the slope and intercept of a linear plot lnK_c versus 1/T.[4,37,38]

$$\Delta G^O = \Delta H^O - T\Delta S^O \quad (6)$$

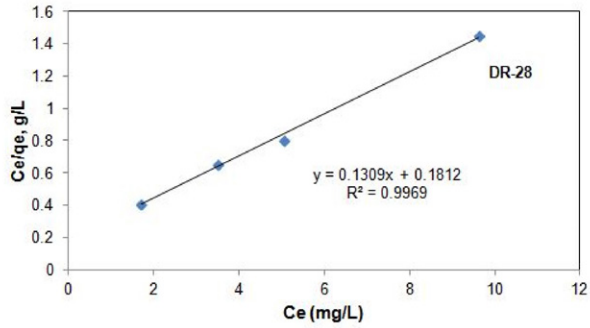

Fig. 10. Langmuir isotherm for DR-28 onto KZF (pH: original, temperature: 21 °C, adsorbent: KZF, adsorbent amount: 1 g/200mL)

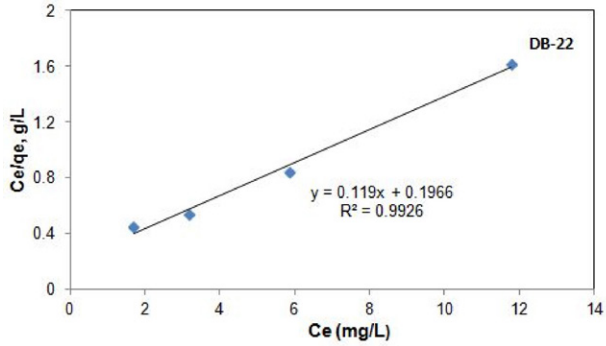

Fig. 11. Langmuir isotherm for DB-22 onto KZF (pH: original, temperature: 40 °C, adsorbent: KZF, adsorbent amount: 1 g/200mL)

$$\ln K_C = -\frac{\Delta G^O}{RT} = \frac{\Delta S^O}{R} - \frac{\Delta H^O}{RT} \quad (7)$$

$$K_C = \frac{q_e}{C_e} \quad (8)$$

where ΔG^0 is the standard change free Gibbs energy (J/mol), ΔH^0 is the standard change enthalpy (J/mol), ΔS^0 is the standard change entropy (J/molK), and R is the universal gas constant (8.314 J/molK), K_c is the ratio of the equilibrium concentration of adsorbate (q_e) loaded to the equilibrium concentration in solution (C_e).

The adsorptions of DR-28 and DB-22 on KZF were thermodynamically studied at an initial concentration of 30 mg/L, with an adsorbent amount of 1g/200mL, and a contact time of 60 min, at the original pH. The results of the thermodynamic study are given in Fig. 12. Table 2 shows the obtained thermodynamic parameters for DR-28 and DB-22.

The enthalpy change (ΔH^0) for DR-28 dyes was found to be –24.59 kJ/mol, which shows that, the adsorption of DR-28 using the composite KZF was exothermic. ΔG^0 values were –1.364, –0.653, 0.137 and 0.927 kJ/mol at the adsorption temperatures of 21, 30, 40, and 50 °C, respectively. The negative ΔG^0 values at 21 and 30 °C indicate that the adsorption process occured spontaneously.[29] The positive ΔG^0 values at 40, and 50 °C suggest that the adsorption of DR-28 onto KZF was not a spontaneous pro-

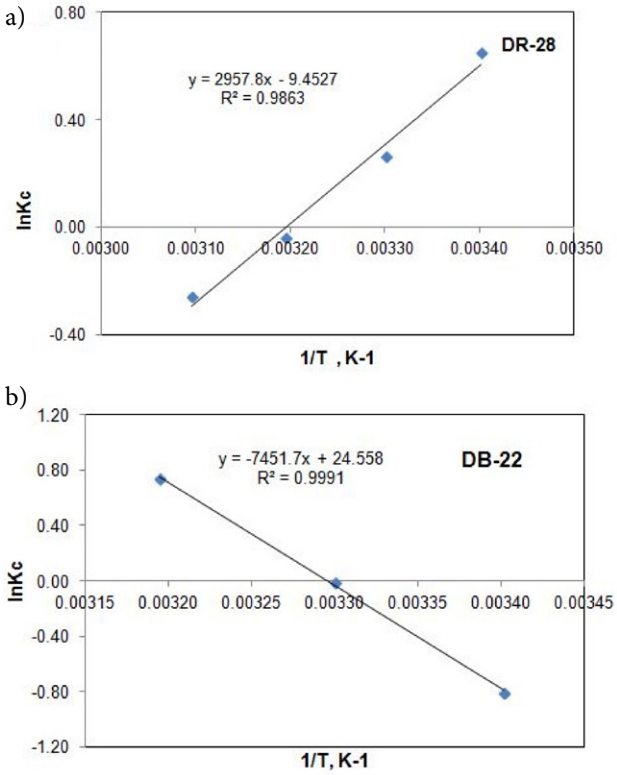

Fig. 12. The thermodynamics of the adsorption of (a) DR-28 and (b) DB-22 on the adsorbent KZF (pH: original, initial concentration: 30 mg/L, contact time: 60 min, KZF amount: 1 g/mL)

cess. The decrease in ΔG^0 value with the decrease in temperature indicates that lower temperatures are suitable for the adsorption of DR-28 molecules onto KZF.[22] The value of ΔS^0 for DR-28 dye was also found to be negative. According to Boushehrian et al.[2], the negative ΔS^0 values indicate a decrease in the random collision of dye molecules and the adsorbent surface during the adsorption process. Maqbool et al.[39] reported similar results for the adsorption of BB-41. The negative value of ΔS^0 reveals that the disorder at the solid-solution interface is reduced.

On the other hand, ΔH^0 value for DB-22 was found to be 61.95 kJ/mol, which shows that the adsorption process was endothermic. ΔG^0 values were 1.974, 0.138, and –1.902 kJ/mol at the adsorption temperatures of 21, 30, and 40 °C, respectively. The positive ΔG^0 value at 21 and 30 °C indicated that the adsorption process was not spontaneous. The negative ΔG^0 value at 40 °C suggests that the adsorption of DB-22 onto KZF was a spontaneous process.[4] The decrease in ΔG^0 value with the increase in temperature shows that higher temperatures are suitable for the adsorption of dye molecules onto adsorbent.[22] As mentioned in the section 3.5 there was no increase in the removal rate of dye beyond 40 °C. So, there is no need to work at temperatures higher than 40 °C. ΔS^0 was found to be 204 J/mol. The positive ΔS^0 shows the increase in disorder and randomness at the composite KZF and DB-22 dye solution interface during the adsorption process.[19,40]

Table 2. Thermodynamic parameters for the adsorptions of DR-28 and DB-22 onto KZF

Dye	Temperature (°C)	ΔH^0 (kJ/mol)	ΔS^0 (J/molK)	ΔG^0 (kJ/mol)
DR–28	21	–24.59	–79	–1.364
	30			–0.653
	40			0.137
	50			0.927
DB–22	21	61.95	204	1.974
	30			0.138
	40			–1.902

3. 9. Adsorption Kinetics

To understand the dynamics of the adsorption process of DR-28 and DB-22 onto KZF, the adsorption kinetic experiments were performed at the adsorbent amount 1g/200mL, with the initial dye concentration of 30 mg/L at original pH. Adsorption temperature was 21 °C for DR-28 and 40 °C for DB-22. Common adsorption kinetic models, pseudo first order equation, and pseudo second order equation were employed to fit the experimental data.

The linear form of the pseudo first order kinetic model is presented as Eq. 9:

$$\ln(q_e - q_t) = \ln q_e - k_1 t \quad (9)$$

In this relation, q_e is the adsorption capacity in the equilibrium state (mg/g), q_t is the adsorption capacity at any time (mg/g), and k_1 is the rate constant (min^{-1}). k_1 can be obtained by drawing the experimental data of $\ln(q_e - q_t)$ versus t.[2,37]

The pseudo second order kinetic model is given in the Eq. 10:

$$\frac{t}{q_t} = \frac{1}{k_2 q_e^2} + \frac{t}{q_e} \quad (10)$$

where k_2 (g/mg.min) is the rate constant of the pseudo second order kinetics. Drawing the linear graph of t/q_t versus t can provide the pseudo second order kinetic rate parameter.[2,37,40]

Regression coefficient (R^2) is important to determine the agreement of calculated q_e values with experimental data. A relatively higher R^2 value indicates that the model is suitable for the adsorption process. The values and constants of the pseudo first order and pseudo second order models for DR-28 and DB-22 are given in Table 3 and Table 4, respectively. The results of the pseudo second order model obtained for the adsorption of DR-28 and DB-22 are shown in Fig. 13 and Fig. 14, respectively.

As can be seen in Table 3 and Table 4, the correlation coefficient (R^2) of the pseudo second order model was

Table 3. Pseudo first order and pseudo second order kinetic model constants for DR-28 adsorption using the adsorbent KZF

Kinetic model	Parameters	Initial dye concentration of DR-28, mg/L			
		20	30	40	50
Pseudo First Order	R^2	0.9531	0.9205	0.9699	0.8018
	k_1	0.0624	0.0783	0.0727	0.0597
	q_{cal}	1.788	3.009	5.385	4.739
	q_{exp}	4.166	5.434	6.266	6.633
Pseudo Second order	R^2	0.9997	0.9980	0.9974	0.9979
	k_2	0.0755	0.0410	0.0195	0.0177
	q_{cal}	4.292	5.692	6.798	7.179
	q_{exp}	4.17	5.43	6.270	6.63

Table 4. Pseudo first order and pseudo second order kinetic model constants for DB-22 adsorption using the adsorbent KZF

Kinetic model	Parameters	Initial dye concentration of DB-22, mg/L			
		20	30	40	50
Pseudo First Order	R^2	0.532	0.8783	0.7863	0.7998
	k_1	0.0467	0.07	0.0464	0.0338
	q_{cal}	0.372	2.749	2.252	2.718
	q_{exp}	3.754	5.831	6.898	7.265
Pseudo Second order	R^2	0.9992	0.9995	0.9993	0.9976
	k_2	0.145	0.049	0.036	0.021
	q_{cal}	3.83	6.05	7.16	7.65
	q_{exp}	3.75	5.83	6.90	7.27

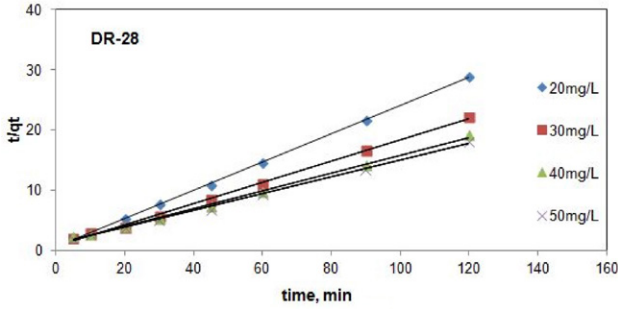

Fig. 13 Pseudo second order model for the adsorption of DR-28 onto KZF

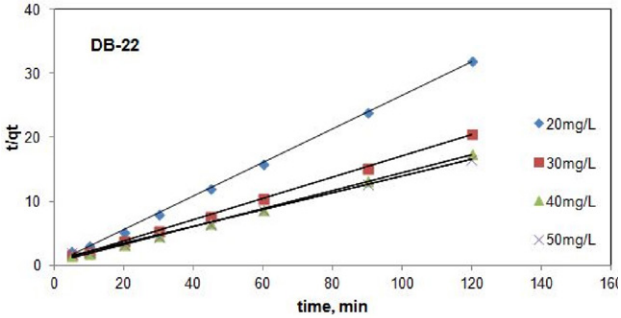

Fig. 14 Pseudo second order model for the adsorption of DB-22 onto KZF

higher than that of the pseudo first order. This result shows that the pseudo second order model is the best model for describing the kinetics of KZF toward DR-28 and DB-22.

4. Conclusion

In this study, the adsorption of diazo dye Direct Red 28 (DR-28) and tetra azo dye Direct Black 22 (DB-22) using synthesized magnetic kaolin supported zinc ferrite (KZF) were investigated. KZF was prepared by co-precipitation method. KZF was heat treated at 200 °C for 3h and coded as KZF-200. KZF provided a higher removal of DR-28 and DB-22 than KZF-200. The characteristics of the KZF and KZF-200 were determined using FTIR, SEM, EDS/Elemental Mapping, XRD, and VSM analyses. The highest removal rates of DR-28 and DB-22 with the composite KZF were obtained at the original pH, at the initial dye concentration of 20mg/L, with the adsorbent amount of 1g/200mL, and the contact time of 120 min, and at 21 °C for DR-28 and 40 °C for DB-22. Under these conditions, the removal rates of DR-28 and DB-22 from aqueous solutions were found to be 92.4% and 91.7% respectively. The experimental results were better fitted with the Langmuir isotherm model and adsorption process occurred on the

homogeneous surfaces. The kinetic behavior of the adsorption of DR-28 and DB-22 showed that the pseudo second-order kinetic model was better fitted with the results. The adsorption of DR-28 using KZF resulted in negative ΔH^0 and ΔS^0 values which indicate exothermic in nature and decrease in random collosion. ΔH^0 and ΔS^0 values for the adsorption of DB-22 using KZF were positive. Adsorption of DB-22 was endothermic. The positive ΔS^0 value indicated the increasing of randomness at the solid/liquid interface during the adsorption.

5. References

1. Y. Zhou, J. Lu, Y. Liu, *Env. Pol.* **2019**, *252*, 352–3659. **DOI:**10.1016/j.envpol.2019.05.072
2. M. M. Boushehrian, H. Hossein Esmaeili, R. Foroutan, *J. Env. Chem. Eng.* **2020**, *8*, 103869. **DOI:**10.1016/j.jece.2020.103869
3. Z. Esvandia, R. Foroutan, J.S. Peighambardoust, A. Akbari, B. Ramavandi, *Surf. and Int*. **2020** *21*, 100754. **DOI:**10.1016/j.surfin.2020.100754
4. M. Fayazi, D. Afzalic, A. Mostafavi, V. K Gupta, *J. Mol. Liq.* **2015**, *212*, 675–685. **DOI:**10.1016/j.molliq.2015.09.045
5. S. Benkhaya, S. M'rabet, A. El Harfi, A., *In. Chem. Com*. **2020**, *115*, 107891. **DOI:**10.1016/j.inoche.2020.107891
6. M. Berradi, R. Hsisou, M. Khudhair, M. Assouag, O. Cherkaoui, A. El Bachiri, A. El Harfi, *Hel.* **2019**, *5*, e02711. **DOI:**10.1016/j.heliyon.2019.e02711
7. S. Benkhaya, S. M'rabet, A. El Harfi, *Hel.* **2020**, *6*, e03271. **DOI:**10.1016/j.heliyon.2020.e03271
8. B. Meroufel, O. Benali, M. Benyahia, Y. Benmoussa, M. A. Zenasni, *J. Mat. Env. Sc.* **2013**, *4(3),* 482–491.
9. N. T. Hien, L. H. Nguyen, H. T. Van, T. D. Nguyen, T. H. V. Nguyen, T. H. H. Chu, T. V. Nguyen, V. T. Trinh, X. H. Vu, K. H. H. Aziz, *Sep. Pur. Tech.* **2020**, *233*, 115961. **DOI:**10.1016/j.seppur.2019.115961
10. H. Patel, R. T. Vashi, *J. Sa. Chem. Soc.* **2012**, *16*, 131–136. **DOI:**10.1016/j.jscs.2010.12.003
11. R. Saleh, A. Taufik, *Sep. Pur. Tech.* **2019**, *210*, 563–573. **DOI:**10.1016/j.seppur.2018.08.030
12. M. Khadhraoui, H. Trabelsi M. Ksibi, S. Bouguerra, B. Elleuch, *J. Haz. Mat*. **2009**, *161*, 974–981. **DOI:**10.1016/j.jhazmat.2008.04.060
13. F. H. AlHamedi, M. A. Rauf, S. S. Ashraf, *Des.* **2009**, *239*, 159–166. **DOI:**10.1016/j.desal.2008.03.016
14. N. Guy, S. Çakar, M. Özacar, *J. Coll. Int. Sc.* **2016**, *466*, 128–137. **DOI:**10.1016/j.jcis.2015.12.009
15. M. Hu, X. Yan, X. Hu, J. Zhang, R. Feng, M. Zhou, *J. Coll. Int. Sc.* **2018**, *510*, 111–117. **DOI:**10.1016/j.jcis.2017.09.063
16. A. Kanwal, H. N. Bhatti, M. Iqbal, S. Noreen, *Wat. Env. Res.* **2017**, *89(4)*, 301–311. **DOI:**10.2175/106143017x14839994522984
17. Z. Gao, X. Li, H. Wu, H. Zhao, W. Deligeer, S. Asuha, *Mic. Mes. Mater.* **2015**, *202*, 1–7. **DOI:**10.1016/j.micromeso.2014.09.029
18. Z. Chen, Y. Cheng, Z. Chen, M. Megharaj, R. Naidu, *J. Nanopart. Res.* **2012**, *14:899*, 1–8. **DOI:**10.1007/s11051-012-0899-0
19. A. Magdy, Y. O. Fouad, M. H. Abdel-Aziza, A. H. Konsowa, *J. Ind. Eng. Chem.* **2017**, *56*, 299–311. **DOI:**10.1016/j.jiec.2017.07.023
20. F. Sun, Q. Zeng, W. Tian, Y. Zhu, W. Jiang, *J. Env. Chem. Eng.* **2019**, *7*, 103011. **DOI:**10.1016/j.jece.2019.103011
21. S. J. Olusegun, N. D. S. Mohallem, *Env. Poll.* **2020**, *260*, 114019. **DOI:**10.1016/j.envpol.2020.114019
22. Q. Huang, M. Liu, J. Chen, K. Wang, D. Xu, F. Deng, H. Huang, X. Zhang, Y. Wei, *J.Mat. Sci*. **2016**, *51*, 8116–8130. **DOI:**10.1007/s10853-016-0082-6
23. A. H. Jawad, A. S. Abdulhameed, *Surf. Int*. **2020**, *18*, 100422. **DOI:**10.1016/j.surfin.2019.100422
24. S. Niu, X. Xie, Z. Wang, L. Zheng, F. Gao, Y. Miao, *Env. Tech*. **2021**, *42(10)*, 1472–1481. **DOI:**10.1080/09593330.2019.1670269
25. D. Ar Rahim, W. Fang, G. Zhu, H. Wibowo, D. Hantoko, Q. Hu, H. Susanto, Z. Gao, M. Yan, *Chem. Eng. Proc.-Pr. Int*. **2021**, *68*, 108565. **DOI:**10.1016/j.cep.2021.108565
26. D. L. Rossatto, M. S. Netto, S. L. Jahn, E. S. Mallmann, G. L. Dotto, E. L. Foletto, *J. Env. Chem. Eng.* **2020**, *8*, 103804. **DOI:**10.1016/j.jece.2020.103804
27. R. Nicola, S-G. Muntean, M-A. Nistor, A-M. Putz, L. Almasy, L. Sacarescu, *Chemos*. **2020**, *261*, 127737. **DOI:**10.1016/j.chemosphere.2020.127737
28. A. Souri, F. Golestani-Fard, R. Naghizadeh, S. Veiseh, *App. Cl. Sci*. **2015**, *103*, 34–39. **DOI:**10.1016/j.clay.2014.11.001
29. C. Cao, L. Xiao, C. Chen, X. Shi, Q. Cao, L. Gao, *Pow. Tech*. **2014,** *260*, 90–97. **DOI:**10.1016/j.powtec.2014.03.025
30. P. Karthikeyan, S. Meenakshi, *Int. J. Bio. Mac.* **2021**, *168*, 750–759. **DOI:**10.1016/j.ijbiomac.2020.11.132
31. P. Koohi, A. Rahbar-kelishami, H. Shayesteh, *Env. Tech. Inn*. **2021**, *23*, 101559. **DOI:**10.1016/j.eti.2021.101559
32. N. M. Mahmoodi, F. Najafi, S. Khorramfar, F. Amini, M. Arami, *J Haz Mat*. **2011**,*198*, 87–94. **DOI:**10.1016/j.jhazmat.2011.10.018
33. R. Das, M. Bhaumik, S. Giri, A. Maity, *Ult. Son*. **2017**, *37*, 600–613. **DOI:**10.1016/j.ultsonch.2017.02.022
34. D. Sun, X. Zhang, Y. Wu, X. Liu, *J. Haz. Mat*. **2010**, *181*, 335–342. **DOI:**10.1016/j.jhazmat.2010.05.015
35. M. Maqbool, S. Sadaf, H. N. Bhatti, S. Rehmat, A. Kausar, S. A. Alissa, M. Iqbal, *Surf and Int*. **2021,** *25*, 101183. **DOI:**10.1016/j.surfin.2021.101183
36. M. M. S. Sanad, M.M. Farahat, M. A. Abdel Khalek, *Adv. Pow. Tech*. **2021**, *32*, 1573–1583. **DOI:**10.1016/j.apt.2021.03.013
37. R. Salahshour, M. Shanbedi, H. Esmaeili, *Acta Chim. Slov*. **2021**, *68*, 363–373. **DOI**:10.17344/acsi.2020.6311
38. T. A. Aragaw, F. T. Angerasa, *Hel.* **2020**, *6*, e04975. **DOI:**10.1016/j.heliyon.2020.e04975
39. M. Maqbool, H. N. Bhatti, S. Sadaf, M.M. AL-Anazy, M. Iqbal, *J Mat. Res. Tech.* **2020**, *9(6)*,14729e14741. **DOI:** 10.1016/j.jmrt.2020.10.017
40. A. Jabeen, H. N. Bhatti, *Env. Tech and Inn.***2021**, 23, 101685 **DOI:** 10.1016/j.eti.2021.101685

Povzetek

Prisotnost molekul barvil v vodah ima škodljiv vpliv na okolje. Zato je pomembno, da jih odstranimo s pomočjo okolju prijaznih materialov. V tej študiji smo preučevali možnost odstranjevanja diazo barvila Direct Red 28 (DR-28) in tetraazo barvila Direct Black 22 (DB-22) z adsorpcijo na kompozitni nosilec na osnovi kaolina in cinkovega ferita (KZF). Lastnosti KZF kompozita smo določili s pomočjo FTIR, SEM, XRD, VSM in EDS. Adsorpcijo barvil DR-28 in DB-22 na KZF smo preučevali v odvisnosti od kontaktnega časa, začetne koncentracije barvila, količine adsorbenta, temperature, začetne pH vrednosti raztopine ter toplotne obdelave kompozita. Dosegli smo 92.4 % adsorpcijo DR-28 pri KZF koncentraciji 1g/200 mL, začetni koncentraciji barvila 20 mg/L, kontaktnem času 120 min, pri osnovni pH vrednosti in temperaturi 21 °C. Adsorpcija barvila DB-22, pri enakih pogojih le temperaturi 40 °C, pa je bila 91.7 %. Rezultati so pokazali, da je lahko adsorpcijo obeh barvil (DR-28 in DB-22) na KZF opišemo z Langmuirjevo adsorpcijsko izotermo. Adsorpcija barvila DR-28 je eksotermna, medtem ko je adsorpcija barvila DB-22 endotermna. Sprememba entalpije (ΔH^0) pri adsorpciji na KZF je bila 24.59 kJ/mol za DR-28 in 61.95 kJ/mol za DB-22. ΔS^0 adsorpcije je bila pri DR-28 negativna, pri DB-22 pa pozitivna. Hitrost adsorpcije obeh barvil lahko dobro opišemo s kinetiko pseudo-drugega reda. Rezultati kažejo, da lahko pripravljeni KZF kompozit uporabimo za učinkovito odstranjevanje anionskih barvil.